

# Nanoscale

Accepted Manuscript



This is an *Accepted Manuscript*, which has been through the Royal Society of Chemistry peer review process and has been accepted for publication.

*Accepted Manuscripts* are published online shortly after acceptance, before technical editing, formatting and proof reading. Using this free service, authors can make their results available to the community, in citable form, before we publish the edited article. We will replace this *Accepted Manuscript* with the edited and formatted *Advance Article* as soon as it is available.

You can find more information about *Accepted Manuscripts* in the [Information for Authors](#).

Please note that technical editing may introduce minor changes to the text and/or graphics, which may alter content. The journal's standard [Terms & Conditions](#) and the [Ethical guidelines](#) still apply. In no event shall the Royal Society of Chemistry be held responsible for any errors or omissions in this *Accepted Manuscript* or any consequences arising from the use of any information it contains.

Cite this: DOI: 10.1039/c0xx00000x

www.rsc.org/xxxxxx

**PAPER**

# Simple, Green and High-yield Production of Single- or Few-layer Graphene by Hydrothermal Exfoliation of Graphite

Xiangrong Liu,<sup>b</sup> Mingtao Zheng,<sup>\*a</sup> Ke Xiao,<sup>b</sup> Yong Xiao,<sup>a</sup> Chenglong He,<sup>b</sup> Hanwu Dong,<sup>a</sup> Bingfu Lei<sup>a</sup> and Yingliang Liu,<sup>\*a</sup>

Received (in XXX, XXX) Xth XXXXXXXXX 20XX, Accepted Xth XXXXXXXXX 20XX

DOI: 10.1039/b000000x

Graphene is widely used as the future electronic materials and devices, owing to its exceptional electronic and optoelectronic properties. Up to now, the defect-free graphene is limited to the method for controllable, reproducible and scalable mass production. A simple, green, and nontoxic approach for the large-scale preparation of high quality graphene is produced by exfoliation of graphite sheets collaborated with intercalant (FeCl<sub>2</sub>) under hydrothermal condition, the absence of defects or oxides graphene with yields up to 10 wt% can be practical application and industrial process such as optical limiters, transparent conductors, and sensors. This new process could potentially be improved to give yields of up to 35 wt% of the starting graphite mass with sediment recycling. We show with experiments and theories that exfoliation graphene is the result of combined action by diminishing the van der Waals interactions between graphite layers and the shear force drove by Brownian motion of H<sub>2</sub>O and FeCl<sub>2</sub> molecules. Hydrothermal exfoliation has potential applications in exfoliation other layered materials (e.g. BN, MoS<sub>2</sub>) and carbon nanotubes, and in synthesis intercalation compounds, nanoribbons, and nanoparticles, thus opens new ways of exfoliation engineering.

## Introduction

Graphene, a one-atom-thick planar sheet of sp<sup>2</sup> hybridised carbon arranged in a honeycomb crystal lattice, has attracted appreciable attention to apply in many technological fields such as nanoelectronics,<sup>1,2</sup> sensors,<sup>3,4</sup> nanocomposites,<sup>5,6</sup> batteries,<sup>7</sup> supercapacitors, and hydrogen storage,<sup>8</sup> due to its exceptional properties including high current density, ballistic transport, chemical inertness, superior thermal conductivity, optical transmittance, biocompatibility and super hydrophobicity.<sup>9,10</sup> However, as with many novel materials, the development and widespread application of graphene are mainly hampered by the lack of methods for controllable, reproducible and scalable mass production.

Since graphene was first prepared by a micro-mechanical cleavage that was realized by simply attaching a scotch tape onto graphite face in 2004,<sup>11</sup> the synthesis of graphene has become one of the most active directions towards obtaining high quality products at a large scale. Although this method is simple in the preparation, it remains challenging to obtain a single layer of graphene and scale up for a practical application.<sup>12</sup> Since then, many physical and chemical methods have been reported, such as chemical vapour deposition, epitaxial growth, oxidation-

reduction of graphite, facile exfoliation and thermal exfoliation.<sup>13-16</sup> Although bottom-up approach including chemical vapor deposition growth and epitaxial growth of graphene onto metal catalyst substrates, large-area and defect-free graphene sheets including a single layer have been achieved, the resulting graphene sheets are generally not freestanding, difficultly transferred to different substrates and the high temperature of preparation. On the other hand, top-down approach which consists of exfoliation of natural or synthetic graphite to single or few layer graphene, including micromechanical cleavage, reduction of graphite oxide,<sup>17,18</sup> electrochemical lithium intercalation<sup>19</sup>, liquid sonication,<sup>20-22</sup> and exfoliation<sup>23-27</sup> have been extensively used for production of graphene. Among those, to obtain defect-free, large-area and high electronic conductivity graphene, the exfoliation graphene serve as the most viable option for the scalable mass production owing to its low cost and ease of solution processing. A number of research groups have studied and reported the production of single and few layer graphene sheets by exfoliation and stabilisation of graphene that are without defects or defect formation in a variety of special solvents.<sup>25-28</sup> Although recently Umar Khan et al. had managed to improve the yield of the solvent exfoliation method up to ~ 1 mg mL<sup>-1</sup>, it required long sonication time of up to 460 hours.<sup>25</sup> However, these solvent exfoliation methods is that the yield was still relatively low, typically at 0.01 mg mL<sup>-1</sup>, which is the critical hamper for practical application. In addition, solvents such as N-methylpyrrolidone (NMP) and dimethylformamide (DMF) are

<sup>a</sup> College of Science, South China Agricultural University, Guangzhou 510642, China, E-mail: mtzheng@scau.edu.cn, tliuyi@163.com,

<sup>b</sup> Department of Chemistry, Jinan University, Guangzhou 510632, P.R. China.

undesirable and further limited the application due to its high boiling point, toxicity, incompatibility with other aspects of processing.

Herein, we studied the possibility of exfoliating graphene in water in the presence of intercalants and surfactant stabilizers under hydrothermal stirring condition. The molecule of H<sub>2</sub>O and FeCl<sub>2</sub> can interact favourably with graphite to diminish van der Waals interactions between graphite layers, thus graphene can be exfoliated from graphite by vigorous Brownian motion of molecule under hydrothermal conditions. Compared to organic solvent exfoliate<sup>25-28</sup>, hydrothermal exfoliation is simple, green, high yield, and nontoxic. Our method results in defect-free single- or few-layer graphene at yields of ~ 10 wt%, the process could potentially be improved to give yields of up to 35 wt% of the starting graphite mass with sediment recycling.

## Experimental section

### Materials and methods

Raw pyrolytic graphite was purchased from Alfa Aesar. Sodium dodecylbenzenesulfonate (SDBS), ferrous chloride (FeCl<sub>2</sub>) were purchased from Sigma Aldrich. All the chemicals and reagents were used as received without any further purification. Graphite was exfoliated in solution that is comprised of water, graphite, SDBS, ferrous chloride corresponding with the weight ratio of 150:2:(0~1):(0~2), and 300:4:5:2 is the optimized ratio in our experience. In order to exfoliate graphite in the hydrothermal condition, above solution was fed into a reactor which is made of 316SS stainless steel with a stirrer, and pure N<sub>2</sub> replaces the air in the reactor. Then, the closed reactor was heated to hydrothermal condition (513 ± 60 K, 30 ± 15 bar), and stirred at 500-1000 rpm for 4-10 hours. After hydrothermal exfoliation, the dispersions were transferred to vials and centrifuged at 500-800 rpm for 10 min using an Allegra 64R centrifuge (Beckman Coulter; 500-10000 rpm for the centrifugation-rate experiment). After centrifugation, the top 135 mL supernatant (out of 150 mL) was carefully collected for further use, and the sediment can be cycled for next hydrothermal exfoliation. By centrifuging the collected supernatant at 8000-1000 rpm, we separated graphene flakes into the bottom of vial from the collected supernatant, and removed supernatant. The separated graphene flakes were washed with distilled water by centrifugation, this procedure was repeated a number of times until SDBS and FeCl<sub>2</sub> removed completely.

### Characterization

We characterized the morphological features of the graphite and graphene by Philips SEM-XL30S scanning electron microscope (SEM) and Philips TECNAI 10 transmission electron microscopy and JEOL JEM52100F field emission electron microscope equipped with an Oxford INCA Energy TEM 200 EDS system. Atomic force microscopy (AFM) images were taken in tapping mode with the SPM Dimension 3100 from Veeco under ambient conditions. Raman spectra of the samples were measured by a Renishaw inVia microspectrometer using an excitation wavelength of 514 nm generated by an Ar<sup>+</sup> laser. Crystallographic phases of the products (XRD) were conducted on a Bruker D8-Advance powder X-ray diffractometer with Cu K $\alpha$  radiation ( $\lambda=0.15418$  nm). Fourier transform infrared (FTIR)

spectra were recorded by an Equinox 55 (Bruker) spectrometer with the KBr pellet technique ranging from 500 to 4000 cm<sup>-1</sup>. The N<sub>2</sub> adsorption-desorption isotherms of the samples were measured at 77 K using Micromeritics ASAP 2020 Analyzer for determining their specific surface area. The specific surface area was calculated from the Brunauer-Emmett-Teller (BET) plot of the nitrogen adsorption isotherm.

## Results and discussion

### 65 Hydrothermal parameter of exfoliation graphene

It is clear that graphite can be dispersed in some solvents. The graphite is almost completely exfoliated to multilayer graphene in NMP,  $\gamma$ -butyrolactone and 1,3-dimethyl-2-imidazolidinone. Thus, many research groups studied solvent properties lead to exfoliate graphite, suggested successful solvents to be those with surface energy close to that of the graphene.<sup>26-29</sup> Such exfoliation can only occur if the net energetic cost is very small. In chemistry, this energy balance is expressed as the enthalpy of mixing (per unit volume), which we can approximately calculate in this case to be the Hildebrand - Scratchard equation (1),<sup>26-29</sup> where  $E_{S,S}$  and  $E_{S,G}$  are the solvent and graphene surface energy, respectively,  $T_{flake}$  is the nanosheet thickness, and  $\Phi_G$  is the dispersed graphene volume fraction. This equation shows the enthalpy of mixing is dependent on the balance of graphene and solvent surface energies. For graphite, the surface energy is defined as the energy per unit area required to overcome the van der Waals forces when peeling two sheets apart. Assuming that the dispersed graphene concentration ( $C_G \propto \Phi_G$ ) should be described by equation (2), where  $D_G$  is the diameter of a graphene sheet ( modeling it as a disk).<sup>27</sup> Here, the approximation  $(x - a)^2 \approx 4a(\sqrt{x} - \sqrt{a})^2$  is used which is reasonably accurate so long as the full width at half maximum of the resulting Gaussian is less than about half the centre value.

$$\frac{\Delta H_{mix}}{V_{mix}} \approx \frac{2}{T_{flake}} (\sqrt{E_{S,S}} - \sqrt{E_{S,G}})^2 \times \phi_G \quad (1)$$

$$C_G \propto \exp \left[ -\frac{\pi D_G^2}{8 E_{S,G} k T} (E_{S,S} - E_{S,G})^2 \right] \quad (2)$$

The enthalpy of mixing is minimized for solvents with surface energies close to that of graphene, suggesting a surface energy of graphene of ~ 68 mJ m<sup>-2</sup> according to calculation and the previous studies.<sup>26-29</sup> Herein, it expects that a minimal energy cost of exfoliation for solvents whose surface energy matches that of graphene. Coupled with the literature, it suggests that not only is the enthalpy of mixing for graphite dispersed in good solvents very close to zero, but the solvent-graphite interaction is van der Waals rather than covalent. In addition, it predicts that good solvents are characterized by surface tensions in the region of 35-45 mJ m<sup>-2</sup>.<sup>26</sup> Coleman et al. found that the dispersed concentration peaked for solvents such as N-methyl-pyrrolidone (NMP) and dimethylformamide (DMF) with surface tensions close to 40 mJ m<sup>-2</sup>, which is equivalent to surface energies of ~70 mJ m<sup>-2</sup>.<sup>26-29</sup>

Normally, for one solid surface, the smaller surface tension of

liquid has the smaller contact angle formed at the solid-liquid interface at the same condition of temperature. When the liquid and solid are mixed, the smaller surface tension of the interface has greater force and penetration which can make solid object swelling. The volume of most substances will expand with rising the temperature, resulted in the distance between molecules increased and the interaction of molecules decreased. Thus, most of the surface tension of the material decreases with increasing temperature. Under the critical temperature (existence of gas-liquid interface), surface tension is inverse linear relationship with temperature. In the colloid solution, the surface tensions ( $\gamma$ ) is identical to the excess Gibbs free energy per unit area arising from the surface ( $G^s$ ). According to thermodynamic function (3), (4) and (5),<sup>30,31</sup>

$$G^s = \gamma = H^s - TS^s \quad (3)$$

$$\left(\frac{\partial G^s}{\partial T}\right)_P = \left(\frac{\partial \gamma}{\partial T}\right)_P = -S^s \quad (4)$$

$$\gamma = H^s + T\left(\frac{\partial \gamma}{\partial T}\right)_P \quad (5)$$

For water,  $H^s$  is about  $117.3 \text{ mJ m}^{-2}$  and  $\partial\gamma/\partial T$  is about  $-0.152 \text{ mJ m}^{-2} \text{ K}^{-1}$ .<sup>30,31</sup> In the closed system, liquid water and water vapor are both present under the supercritical temperature (547 K, 22.4 MPa).<sup>32</sup> Because the closed reactor system only has energy exchange and the external pressure of the closed reactor system is constant, the temperature is the most fundamental factor of surface tension and pressure. So the influence of pressure for surface tension in the thermodynamic equation was neglected. Herein, the surface tension of water can be given under 547 K in the closed system. Surface tensions in the region of  $35\text{--}45 \text{ mJ m}^{-2}$  are consistent with the temperatures in the region of  $475\text{--}541 \text{ K}$  in the sealed reaction vessel. In our experiments, the surface tensions of water close to  $40 \text{ mJ m}^{-2}$  at hydrothermal condition (about 513 K, 3.0 MPa) to obtain quantitative yield of  $\sim 4 \text{ wt\%}$  (see Supplementary Information, Fig. S1).

In order to avoid the dispersed graphene aggregating, surfactants such as SDBS, sodium dodecyl sulfate and sodium cholate are employed to disperse graphene in the process of refrigeration of hydrothermal system. To further improve the yield of graphene, intercalated graphite could be exfoliated by reactions involving the intercalant.<sup>33</sup> It is expected that intercalant can intercalate into graphene sheet to diminish van der Waals interactions between graphite layers and graphene sheets are dispersed in subcritical water. Meanwhile, intercalant can be dissolved in water and washing the production without affecting the purity of graphene. According to literature,<sup>33-35</sup> alkali metal, metal halide and acid are employed to intercalate graphite layers. Among intercalants,  $\text{FeCl}_2$  that is soluble in water and nontoxicity is an intercalant of acceptor type.<sup>33,34</sup> In our experiment, the removed supernatant can detect the existence of  $\text{Fe}^{2+}$  by colour reaction with alkali,  $\text{FeCl}_2$  is conducted to auxiliary exfoliation of graphite. Our method results in high-quality, unoxidized single- and few-layer graphene at yields of  $\sim 10 \text{ wt\%}$  (see Supplementary Information, Fig. S1). In fact, we also find that the sediment can

be recycled to produce dispersions with mass fractions of graphene that we have measured to be  $\sim 35 \text{ wt\%}$ , respectively.

### Evidence and identification of single- or few-layer graphene

X-ray diffraction (XRD) patterns were employed to identify graphene, indicating that no structure changes occurred during hydrothermal exfoliation process (see Supplementary Information, Fig. S2). The interlayer diffraction (002) peak of exfoliated graphite clearly downshifts compared to pristine graphite compared to pristine graphite, and a dramatical decrease in the intensity of (002) peak of graphite can be observed. As the in-plane crystal structure of graphite retained, the broadening of (002) peak of the exfoliated graphite should be caused by decreased the thickness of graphite. In addition, hydrothermal exfoliation of graphite leads to a dramatically increase in the BET surface area from  $3.6 \text{ m}^2 \text{ g}^{-1}$  for pristine graphite to  $217.3 \text{ m}^2 \text{ g}^{-1}$  for graphene (see Supplementary Information, Fig. S3).

The morphology of initial graphite powder and sediment flakes is examined. Scanning electron microscopy (SEM) studies (Fig. 1a) show the starting powder to consist of flakes of lateral size measured in hundreds of micrometres and thicknesses tens of micrometres. In comparison, the sediment separated after centrifugation contains flakes, which are much smaller, with lateral size  $< 100 \mu\text{m}$  and thickness  $< 15 \mu\text{m}$  (Fig. 1b). Clearly, hydrothermal exfoliation results in fragmentation of the initial flakes, with the largest removed by centrifugation.

It is possible to investigate the state of the material remaining dispersed using transmission electron microscopy (TEM) by dropping a small quantity of dispersion onto the carbon film. Bright-field TEM images of the objects are typically observed in Fig. 1c and d, which generally comprises corrugated and folded graphene layers, few-layer graphene and monolayer graphene. As shown in Fig. 1d, in a number of cases we observe monolayer graphene. In some cases the sheet edges tend to scroll and fold slightly. The number of layers in the graphene can be obtained visually by high-resolution TEM (HRTEM) analysis. Few-layered graphene and monolayer graphene, some of them are folded and stacked up, can also be observed (Fig. 1e). From Fig. 1f, the edge of HRTEM can observe the suspended film that few-layer graphene ( $\sim 4\text{--}6$  layers) can be observed from the fringe of the film edge that are clearly visible.

As we known, atomic force microscopy (AFM) is currently the foremost methods allowing definitive identification of single-layer crystals. AFM images of graphene exfoliated by hydrothermal treatment in water after centrifugation always revealed the presence of sheets with uniform thickness ( $< 2 \text{ nm}$ ; examples are shown in Fig. 2). The step heights measured between the surface of the sheets and the substrate are consistently found to be  $16 \pm 1 \text{ \AA}$  (Fig. 2a) and  $7 \pm 1 \text{ \AA}$  (Fig. 2b), proving them to be only double layers or single layer atoms thick. While, theoretically, a pristine graphene sheet is atomically flat with a well-known van der Waals thickness of  $\sim 0.34 \text{ nm}$ , graphene sheets are expected to be 'thicker' due to instrument interference and error coexistence with the presence of free space between graphene plane and the substrate. Commonly, thickness of graphene film  $< 1 \text{ nm}$  is regarded as monolayer graphene. As shown in Figure 2d, the exfoliated graphene are flat sheets with an average thickness of about  $7.3 \text{ nm}$  and its lateral dimension is about  $1.2 \mu\text{m}$ .

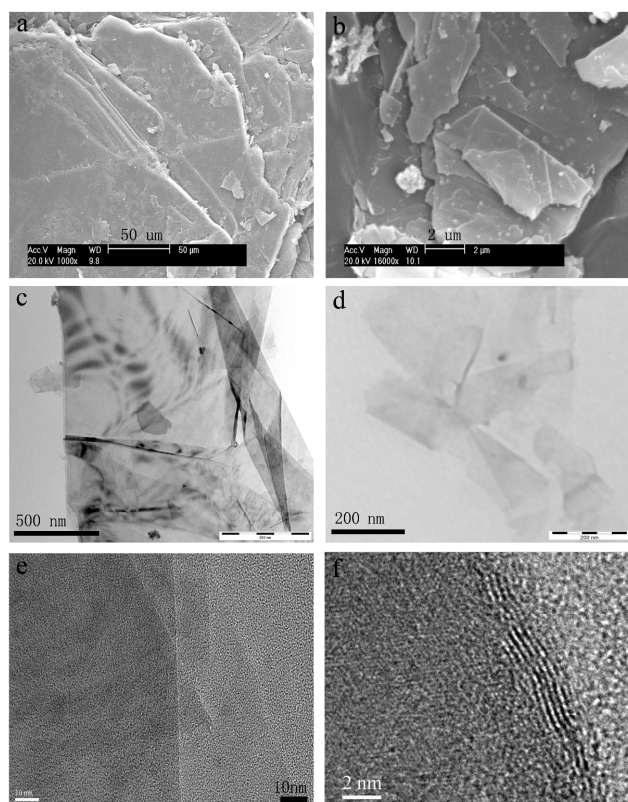


**Fig. 1** Electron microscopy of graphite and graphene. SEM image of pristine graphite (a). SEM image of sediment graphite after centrifugation (b). TEM images of few-layer and folded graphene sheets (c, scale bars: 500 nm), monolayer graphene (d, scale bars: 200 nm), respectively. HRTEM images of folded graphene (e, scale bars: 10 nm). HRTEM images of monolayer or double layers graphene (f, scale bars: 5 nm).

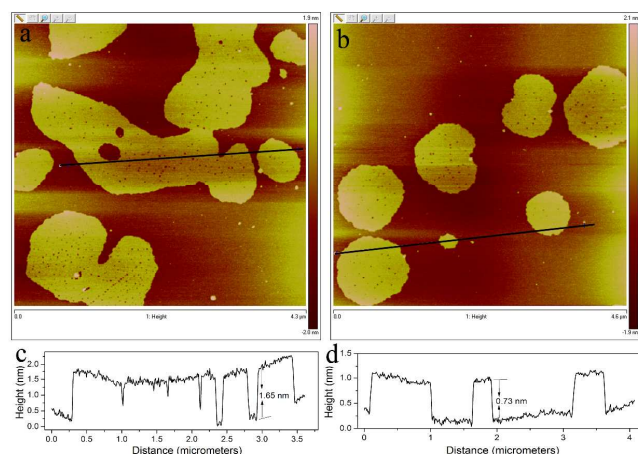


**Fig. 2** Evidence and identification of single- or few-layer graphene. Tapping mode AFM images (a, b) and the corresponding height profiles of the graphenes (c, d). The thicknesses of the graphenes are 1.55–1.67 nm and 0.64–7.5 nm, respectively.

### Evidence for defect-free graphene

Although hydrothermal exfoliated suggests a van der Waals type water – graphene interaction, it is crucial to definitively rule out any inadvertent basal-plane functionalization, which could alter the electronic structure. As shown in Figure 3a, the Raman spectra of the bulk graphite and exfoliated graphene in the range of 600–4000  $\text{cm}^{-1}$  are given. The 1580  $\text{cm}^{-1}$  band (G band),

assigned to the  $E_{2g}$  stretching mode of graphite and reflects the structural intensity of the  $sp^2$ -hybridized carbon atom. The band observed at about 1350  $\text{cm}^{-1}$  is D band, which corresponds to a splitting of the zone center phonons of K-point phonons of  $A_{1g}$  symmetry, characterizes the disordered graphite planes and the defects incorporated into pentagon and heptagon graphitic structures. The minor D band (Figure 3a) of graphene indicates that hydrothermal exfoliation of graphite preserves the honeycomb crystal lattice and structure to obtain defect-free graphene.<sup>20</sup> The result shows that a significant change in relative intensity of the 2D band and G band of graphene compared to pristine graphite. Gupta et al.<sup>36</sup> and Graf et al.<sup>37</sup> have been demonstrated that the relative intensity of the second-order band at 2700  $\text{cm}^{-1}$  is larger than that of the first order-allowed G-band for the number of graphene layers  $< 5$ , and exhibits an interesting layer-dependence. In the Raman spectra, the relative intensity ratio between G band and 2D band of exfoliated graphene is much smaller than pristine graphite, indicating that hydrothermal exfoliation is a feasible approach to exfoliate graphite. Because of stacked, folded and scrolled graphene, it is difficult to obtain the Raman spectra of multi-graphene (the number of layers  $< 5$ ). The Raman spectra of exfoliated graphene collected at different sites (see Supplementary Information, Fig. S4), indicating that there are no obvious differences, and the D peak ( $\sim 1,350 \text{ cm}^{-1}$ ) gives evidence of the presence of defects, that is, either edges.

To study the bonding state of carbon atom in the exfoliated graphene, X-ray photoelectron spectroscopy (XPS), a powerful spectroscopic technique that measures the elemental composition, empirical formula, chemical state and electronic state of the elements existed in a material, was employed to determine the hybridization of the carbons on the surface. The full scan spectra of the graphene and pristine graphite are shown in Figure 3b. The peaks at binding energy of 284.6 eV and 533.15 eV are ascribed to C1s and O1s. The O1s is ascribed to the adsorbed molecular oxygen on the surface of the graphene and pristine graphite. As shown in Figure 3b insert, only a pronounced C1s peak at 284.6 eV can be observed in the XPS spectra of exfoliated graphene, indicating high purity of the exfoliated graphene sample. The C1s XPS spectra of graphene clearly reveal that the intrinsic in-plane crystal structure of graphite remains intact during hydrothermal exfoliation process.

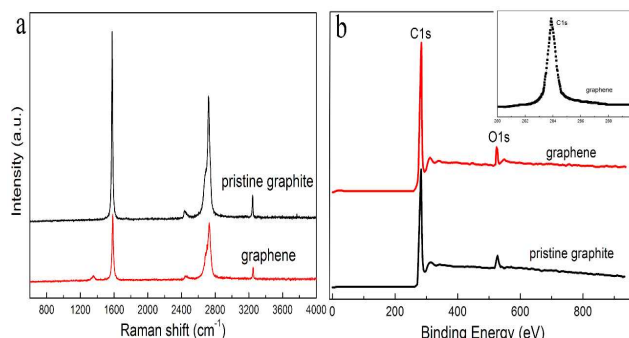


**Fig. 3** Evidence for defect-free graphene. Raman spectra for bulk graphite and exfoliated graphene (a). XPS survey spectra of pristine graphite and exfoliated graphene (b), Insert, a carbon 1s core-level XPS spectrum of graphene (Binding energy: 280–290 eV).

### The possible hydrothermal exfoliation process for graphene

Graphite is stacked layers of many graphene sheets, bonded together by weak van der Waals force. Thus, in principle, it is possible to produce graphene from a high purity graphite sheet, if these bonds can be broken. Theoretical simulations suggested that polar molecules such as aminotriazines can be adsorbed on the graphite through specific interactions of  $\text{NH}_2$  groups with the underlying surface of graphite.<sup>38</sup> Researchers had revealed that the van der Waals force between the two water molecules is decreased with increasing of temperature in the condition of high-temperature-high-pressure, indicating the water molecules are force-free and have vigorous Brownian motion of molecule under hydrothermal conditions.<sup>32,39,40</sup> Interesting,  $\text{H}_2\text{O}$  is polar molecules of V-shaped structure and the surface tensions of water close to  $40 \text{ mJ m}^{-2}$  at hydrothermal condition, suggesting that water molecules can be adsorbed on graphite sheets and dispersed graphene. Molecules of V-shaped structure can easily to embed the graphite layers, and separate the flakes. The additive of  $\text{FeCl}_2$  plays a key role on the exfoliation of graphite to form few layer graphene. The presence of  $\text{FeCl}_2$  after hydrothermal treatment can be certified by FTIR analyses (see Supplementary Information, Fig. S5). During the process,  $\text{FeCl}_2$  act as an intercalant can intercalate into graphene sheet to diminish van der Waals interactions between graphite layers and graphene sheets in subcritical water. We propose the interaction between  $\text{H}_2\text{O}$ ,  $\text{FeCl}_2$  molecules and graphite particles can facilitate exfoliation of graphene sheets from surface of graphite particles. Due to the interaction between  $\text{H}_2\text{O}$ ,  $\text{FeCl}_2$  molecules and graphite flakes under the condition of hydrothermal, graphite can be exfoliated into few or single-layered graphene sheets upon the shear force drove by Brownian motion of  $\text{H}_2\text{O}$  and  $\text{FeCl}_2$  molecules (Scheme 1). Exfoliated graphene sheets are dispersed by water and surfactant, and centrifuged graphene and sediment.

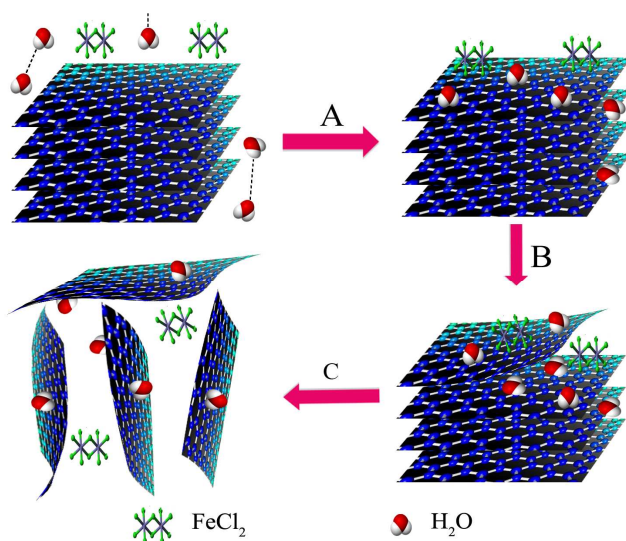


**Fig. 4** Schematic illustration of hydrothermal exfoliation process for graphite flakes in presence of  $\text{H}_2\text{O}$  and  $\text{FeCl}_2$  comprising of three process of A, B, C. The interaction between  $\text{H}_2\text{O}$ ,  $\text{FeCl}_2$  molecules and graphite flakes under the condition of hydrothermal (A). Exfoliation of graphite drove by vigorous Brownian motion of  $\text{H}_2\text{O}$  and  $\text{FeCl}_2$  molecules (B). Exfoliated graphene sheets are dispersed by water and surfactant (C).

## Conclusions

In summary, a hydrothermal exfoliation approach has been developed for production of high quality graphene from exfoliation of graphite sheets collaborated with intercalant ( $\text{FeCl}_2$ ). AFM, Raman spectra, and XPS have demonstrated hydrothermal exfoliation of graphite is simple, green, high yield, and nontoxic method to produce single- or few-layer graphene. Our method results in defect-free graphene at yields of  $\sim 10 \text{ wt}\%$ , the process could potentially be improved to give yields of up to  $35 \text{ wt}\%$  of the starting graphite mass with sediment recycling. In addition,  $\text{FeCl}_2$  can diminish van der Waals interactions between graphite layers, and the molecule of  $\text{H}_2\text{O}$  can be adsorbed/spread on the surface of graphite under hydrothermal condition. Thus, graphite can be exfoliated into few or single-layered graphene sheets upon the shear force drove by Brownian motion of  $\text{H}_2\text{O}$  and  $\text{FeCl}_2$  molecules. Also, exfoliated graphene as a mechanical reinforcement for polymer-based composites can be used for a range of applications such as optical limiters, transparent conductors, and sensors. Furthermore, our approach can, in principle, be used to synthesize intercalation compounds and nanoparticles, and to exfoliate other layered compounds such as BN,  $\text{MoS}_2$ , and carbon nanotubes. This hydrothermal exfoliation technique can be applied to a wide range of materials and has the tremendously potential to be scaled up into an industrial process. We believe this highly efficient method will offer a simple and green approach for the preparation of high quality and large quantity graphene, and open up a range of potential large-area applications, from device and sensor fabrication to liquid-phase chemistry.

This work was supported by the National Natural Science Foundation of China (No. 21031001, 21201065), the Guangdong Higher Education Technology Innovation Key Project (cxzd1014), the National Natural Science Foundation of Guangdong Province, China (s2012040007836), and the Science and Technology Plan Projects of Guangdong Province (2011A081301018).

## References

- P. Avouris, Z. Chen and V. Perebeinos, *Nat. Nanotechnol.*, 2007, **2**, 605–615.
- Y. W. Son, M. L. Cohen and S. G. Louie, *Nature*, 2006, **444**, 347–349.
- F. Schedin, A. K. Geim, S. V. Morozov, E. M. Hill, P. Blake, M. I. Katsnelson and K. S. Novoselov, *Nat. Mater.*, 2007, **6**, 652–655.
- A. Sakhae-Pour, M. T. Ahmadian and A. Vafai, *Solid State Commun.*, 2008, **147**, 336–340.
- S. Stankovich, D. A. Dikin, G. H. B. Dommett, K. M. Kohlhaas, E. J. Zimney, E. A. Stach, R. D. Pinen, S. T. Nguyen and R. S. Ruoff, *Nature*, 2006, **442**, 282–286.
- S. Watcharotone, D. A. Dikin, S. Stankovich, R. Piner, I. Jung, G. H. B. Dommett, G. Evmenenko, S. E. Wu, S. F. Chen, C. P. Liu, S. T. Nguyen and R. S. Ruoff, *Nano Lett.*, 2007, **7**, 1888–1892.
- K. S. Kim, Y. Zhao, H. Jang, S. Y. Lee, J. M. Kim, K. S. Kim, J. H. Ahn, P. Kim, J. Y. Choi and B. H. Hong, *Nature*, 2009, **457**, 706–710.
- K. S. Novoselov, D. Jiang, F. Schedin, T. J. Booth, V. V. Khotkevich, S. V. Morozov and A. K. Geim, *Proc. Natl. Acad. Sci. U.S.A.*, 2005, **102**, 10451–10453.
- A. K. Geim and P. Kim, *Sci. Am.*, 2008, **298**, 90–97.
- A. K. Geim and K. S. Novoselov, *Nat. Mater.*, 2007, **6**, 183–191.
- K. S. Novoselov, A. K. Geim, S. V. Morozov, D. Jiang, Y. Zhang, S. V. Dubonos, I. V. Grigorieva and A. A. Firsov, *Science*, 2004, **306**, 666–669.
- M. J. Allen, V. C. Tung and R. B. Kaner, *Chem. Rev.*, 2010, **110**, 132–145.

- 13 A. Reina, X. Jia, J. Ho, D. Nezich, H. Son, V. Bulovic, M. S. Dresselhaus and J. Kong, *Nano Lett.*, 2009, **9**, 30–35.
- 14 S. Stankovich, D. A. Dikin, R. D. Piner, K. A. Kohlhaas, A. Kleinhammes, Y. Jia, Y. Wu, S. T. Nguyen and R. S. Ruoff, *Carbon*, 2007, **45**, 1558–1565.
- 15 W. Gu, W. Zhang, X. Li, H. Zhu, J. Wei, Z. Li, Q. Shu, C. Wang, K. Wang, W. Shen, F. Kang and D. Wu, *J. Mater. Chem.*, 2009, **19**, 3367–3369.
- 16 W. A. D. Heer, C. Berger, X. Wu, P. N. First, E. H. Conrad, X. Li, T. Li, M. Sprinkle, J. Hass, M. L. Sadowski, M. Potemski and G. Martinez, *Solid State Commun.*, 2007, **143**, 92–100.
- 17 S. Stankovich, R. D. Piner, X. Q. Chen, N. Q. Wu, S. T. Nguyen and R. S. Ruoff, *J. Mater. Chem.*, 2006, **16**, 155–158.
- 18 D. Li, M. B. Muller, S. Gilje, R. B. Kaner and G. G. Wallace, *Nat. Nanotechnol.*, 2008, **3**, 101–105.
- 19 J. Z. Wang, K. K. Manga, Q. L. Bao and K. P. Loh, *J. Am. Chem. Soc.*, 2011, **133**, 8888–8891.
- 20 V. Chabot, B. Kim, B. Sloper, C. Tzoganakis and A. Yu, *Sci. Rep.*, 2013, **3**, 1378, DOI: 10.1038/srep01378.
- 21 Choucair, M. and P. Thordarson, *Nat. Nanotechnol.*, 2008, **4**, 30–33.
- 22 D. Nuvoli, L. Valentini, V. Alzari, S. Scognamillo, S. B. Bon, M. Piccinini, J. Illescas and A. Mariani, *J. Mater. Chem.*, 2011, **21**, 3428–3431.
- 23 J. S. Y. Chia, M. T. T. Tan, P. SimKhiew, J. K. Chin, H. Lee, D. Bien, A. Teh and C. W. Siong, *Chem. Eng. J.*, 2013, **231**, DOI: 10.1016/j.cej.2013.06.106.
- 24 L. Liu, Z. Xiong, D. Hu, G. Wu, P. Chen, *Chem. Commun.*, 2013, **49**, 7890–7892.
- 25 U. Khan, A. O'Neill, M. Lotya, S. De, J. N. Coleman, *Small*, 2010, **6**, 864–871.
- 26 Y. Hernandez, V. Nicolosi, M. Lotya, F. M. Blighe, Z. Y. Sun, S. De, I. T. McGovern, B. Holland, M. Byrne, Y. K. Gun'ko, J. J. Boland, P. Niraj, G. Duesberg, S. Krishnamurthy, R. Goodhue, J. Hutchison, V. Scardaci, A. C. Ferrari and J. N. Coleman, *Nat. Nanotechnol.*, 2008, **3**, 563–568.
- 27 J. N. Coleman, *Accounts Chem. Res.*, 2013, **46**, 14–22.
- 28 M. Lotya, Y. Hernandez, P. J. King, R. J. Smith, V. Nicolosi, L. S. Karlsson, F. M. Blighe, S. De, Z. Wang, I. T. McGovern, G. S. Duesberg and J. N. Coleman, *J. Am. Chem. Soc.*, 2009, **131**, 3611–3620.
- 29 J. H. Hildebrand, J. M. Prausnitz and R. L. Scott, *Regular and related solutions* (1st Ed.). Van Nostrand Reinhold Company: New York, 1970.
- 30 P. C. Hiemenz, *Principles of colloid and surface chemistry*; Marcel Dekker INC: New York, 1977, Chapter 6.
- 31 P. W. Atkins, *Physical Chemistry* (6th Ed.), W. H. Freeman and Company: New York, 1997.
- 32 M. Modell, *Processing methods for the oxidation of organics in critical water*; 1985, U.S. Patent. 4,543,190.
- 33 T. Enoki, M. Suzuki and M. Endo, *Graphite intercalation compounds and applications*, Oxford Univ. Press: London, 2003.
- 34 M. S. Dresselhaus and G. Dresselhaus, *Adv. Phys.*, 1981, **30**, 139–326.
- 35 W. J. Zhao, P. H. Tan, J. Liu and A. C. Ferrari, *J. Am. Chem. Soc.*, 2011, **133**, 5941–5946.
- 36 A. Gupta, G. Chen, P. Joshi, S. Tadigadapa, P. C. Eklund, *Nano Lett.*, 2006, **6**, 2667–2673.
- 37 D. Graf, F. Molitor, K. Ensslin, C. Stampfer, A. Jungen, C. Hierold and L. Wirtz, *Nano Lett.*, 2007, **7**, 238–242.
- 38 V. León, M. Quintana, M. A. Herrero, J. L. G. Fierro, A. de la Hoz, M. Prato and E. Vazquez, *Chem. Commun.*, 2011, **47**, 10936–10938.
- 39 K. Byrappa and T. Adschiri, *Prog. Cryst. Growth. Ch.*, 2007, **53**, 117–166.
- 40 K. Byrappa and M. Yoshimura, *Handbook of Hydrothermal Technology* (2nd Ed.), Elsevier: Oxford, 2013.

## Table of Contents Graphic

Schematic illustration of hydrothermal exfoliation of graphite to produce graphene with intercalant and stabilizer under hydrothermal stirring condition.

